Back to the deformation and Stress Change Modeling home page

R. S. Stein, G. C. P. King and J. Lin,
Change in failure stress on the southern San Andreas fault system caused by the 1992 Magnitude=7.4 Landers earthquake, *Science, 258, pp. 1328-1332, 1992*.
[Online Article]

Change in failure stress on the southern San Andreas fault system caused by the 1992 Magnitude=7.4 Landers earthquake

Ross S. Stein, Geoffrey C.P. King, and Jian Lin

The 28 June Landers earthquake brought the San Andreas fault significantly closer to failure near San Bernardino, a site that has not sustained a large shock since 1812. Stress also increased on the San Jacinto fault near San Bernardino and on the San Andreas fault southeast of Palm Springs. Unless creep or moderate earthquakes relieve these stress changes, the next great earthquake on the southern San Andreas fault is likely to be advanced by 1 to 2 decades. In contrast, stress on the San Andreas north of Los Angeles dropped, potentially delaying the next great earthquake there by 2 to 10 years.

The largest earthquake to strike southern California during the past four decades did not rupture the San Andreas fault, but instead slipped faults within the eastern California shear zone identified previously by geologic (1), geodetic (2), and mechanical (3) methods. Here we show that several smaller shocks which occurred near the Landers event during the preceding 17 years increased stress at the future Landers epicentral site and along much of the eventual rupture path. Similarly, we argue that the Landers earthquake and its aftershocks have changed the stress along the San Andreas fault system.

Table 1. *Earthquakes included in the boundary element models.*

Earthquake	Date	Moment-Magnitude	Moment (dyne-cm)	Length (km)	Reference

Galway Lake	31-May-75	5.2	6.3E+23	5	(25)
Homestead Valley	15-Mar-79	5.6	4.2E+24	6	(7, 26)
Imperial Valley	15-Oct-79	6.5	6.0E+25	40	(17)
North Palm Springs	7-Aug-86	6.0	1.1E+25	9	(27, 2)
Superstition Hills	24-Nov-87	6.6	1.1E+26	22	(9,17)
Elmore Ranch	24-Nov-87	6.2	2.5E+25	17	(9, 17)
Joshua Tree	23-Apr-92	6.1	2.2E+25	12	(27)
Landers	28-June-92	7.4	1.1E+27	75	(30, 32)
Big Bear	28-Jun-92	6.5	5.5E+25	18	(31)

We use an elastic-halfspace boundary element model to simulate the immediate static response of the crust to earthquakes. The earthquakes are represented by cuts extending from the ground surface to 12.5 km depth using the parameters in Table 1; stress is sampled half way down the fault. To assess the long-term static response after the lower crust has fully relaxed, ~30-100 years after the earthquake, we use an elastic plane-stress boundary element model, in which the seismogenic zone is treated as a 12.5-km-thick plate (4).

To gauge the change in proximity to failure of faults in the earth's crust, we calculate the change in the Coulomb failure stress, $\Delta\sigma_f$ [ΔCFF in (5)], acting on vertical planes in the crust. Here:

$$\Delta\sigma_f = \Delta\tau_s + \mu(\Delta\sigma_n - \Delta P)$$

where $\Delta\tau_s$ is the static shear stress change (positive in the direction of the regional τ_s) and $\Delta\sigma_n$ is the normal stress change (positive tensile), μ is the static coefficient of friction, and ΔP is the pore pressure change. For

plausible fault zone rheologies (1) may reduce to $\Delta\tau_s + \mu'(\Delta\sigma_n)$, where $\mu' = \mu(1-B)$ and B is Skempton's coefficient, which can range between 0-1 (6). Thus ΔP acts to cancel $\Delta\sigma_n$, and low μ' may be the product of laboratory values of μ (0.75) and high pore fluid pressure (B tends to 1). Coulomb failure stress changes were calculated for the 1979 Homestead Valley (7), 1984 Morgan Hill (8), 1987 Superstition Hills (9) and 1989 Loma Prieta (5, 10) earthquakes, with deduced values of $0.2 \leq \mu' \leq 0.75$. We examined $\mu' = 0.0, 0.4$, and 0.75, but since our conclusions change only in detail by μ' used, the figures illustrate $\mu'=0.4$.

The maximum Coulomb failure stress changes occur on planes optimally aligned for failure. The earthquake stress changes plus the regional stress control the orientation of the optimum failure planes. Because the regional stress driving plate motion is larger than the stress changes caused by fault slip, the regional stress dominates the orientation of the failure planes, except very close to the fault (8). Examples of such planes are shown in Fig. 1 for two regional stress directions, with a uniaxial compression of 100 bars chosen to be larger than typical earthquake stress drops. In the calculations that follow, we assign a regional principal compressive stress of 100 bars oriented N7°E, intermediate between the examples of Fig. 1. N7°E is the orientation of principal strain contraction measured during 1934-1991 across the Landers and southern San Andreas faults (11). It is also the orientation derived from stress inversion of small shocks along the nearest 50-150 km of the San Andreas fault (12).

The direction is consistent with the shear strain direction predicted by the Pacific-North American plate motion in central California (13), but is discordant with the stress orientation measured in the Cajon Pass well close to the San Andreas fault, 100 km west of the Landers earthquake (14). Our results are valid unless the spatial variability of the true stress field is very high.

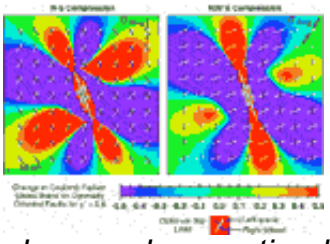

Fig. 1. *Example calculations of the maximum Coulomb failure stress change along optimally oriented right-lateral (black) and left-lateral (white) planes, as a function of the regional stress direction. The regional stress magnitude is 100 bars uniaxial compression. The example fault is 70 km long and 12.5 km deep with 5 m of tapered slip and a stress drop of 85 bars. The coefficient of friction (μ=0.4) controls the angle between the right and left lateral planes and the influence of the normal stress on the Coulomb stress. Near the fault, the optimal planes are rotated because the failure stress change is nearly as large as the regional stress.*

(Click on the diagram to display a large image - 23kb)

The change in Coulomb failure stress caused by the 1975 Galway Lake, 1979 Homestead Valley, 1986 North Palm Springs and 1992 Joshua Tree earthquakes is shown in Fig. 2A (15). Our calculations show that the shocks caused a ~1 bar increase in the proximity to failure of the Landers fault at the future epicenter. Equally important, the failure stress along most of the future 70-km-long Landers rupture rose about 1 bar [for comparison, the Landers earthquake stress drop was ~85 bars (16)]. Thus, although we do not know whether the smaller earthquakes are themselves part of a larger process of earthquake preparation, they raised the stress along the future Landers rupture zone, advancing the occurrence of the Landers earthquake. The failure stress resolved on the Landers rupture plane is greatest when μ is high, but is still favorable for low μ. All four shocks increased the failure stress at Landers, with the Homestead and Joshua earthquakes contributing the most. It was pointed out in 1983 (7) that most aftershocks of the 1979 Homestead Valley earthquake occurred in regions where the Coulomb failure stress was predicted to have increased by >0.3 bar. In addition, geodetic

data suggested that at the site of the future Landers epicenter the fault crept about 10 cm during the 2 years following the Homestead earthquake (7). Thus some parts of the Landers fault were apparently near failure 12 years ago; two months before the Landers rupture, the Joshua Tree earthquake further increased the stress.

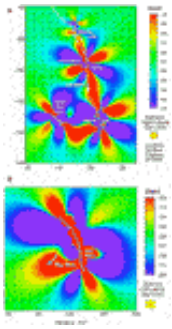

Fig. 2. *(A) Failure stress changes (μ=0.4) caused by the four ML?5.2 shocks within 50 km of the Landers earthquake occurring during 17 yr before the right-lateral Landers rupture. The Landers surface rupture tends to lie within the zone of elevated stress change, and is favorably oriented for right-lateral failure (black lines). Upper left corner is at 34.64°N/116.84°W; lower left corner is at 33.75°/116.08°W. (B) Failure stress changes (μ=0.4) preceding the left-lateral Big Bear aftershock of the Landers earthquake. The stress change at the Big Bear epicenter is 3.0 bars and is optimally oriented for left-lateral failure (white lines). The Landers rupture is divided into 11 slip segments from preliminary fault mapping (32) and seismic analyses (31). From north to south, assigned Landers slip segments are: 1.0, 2.0, 3.0, 4.0, 6.0, 8.0, 5.0, 3.5, 5.0, 3.5, and 0.25 m. Upper left corner is at 35.00°N/117.44°W; lower left corner is at 33.66°N/115.70°W.*

(Click on the diagram to display a large image - 33kb)

The same process of stress transfer can be observed with the apparent triggering of the Big Bear earthquake 3 hr 26 min after the Landers shock. The Landers rupture is predicted to have increased the proximity to failure at the Big Bear epicenter by 3 bars (Fig. 2B). The stress change at Big bear increases for high μ . The rupture plane of the Big Bear shock is optimally aligned for failure, lies in the largest lobe of enhanced Coulomb failure stress resulting from the Landers event, and terminates where the failure stress change becomes negative. Aftershocks during 25 days after the main shock occur in regions where the failure stress increased by ≥ 0.1 bar (Fig. 3). Even when earthquakes within 5 km of the Landers, Big Bear and Joshua Tree faults are excluded, more than 75% of the remaining aftershocks occur where the stress is predicted to have increased by ≥ 0.5 bar. In contrast, less than 25% violate our prediction and occur where the stress dropped by ≥ 0.5 bar. Faults predicted to have been loaded by the Landers rupture include the San Jacinto, Camp Rock, Lenwood, Blackwater, Pisgah and eastern Garlock faults, all of which show Landers aftershocks. An exception occurs near Indio, where the San Andreas has been loaded both by the Landers earthquake and, to a lesser extent, by the Imperial Valley, Elmore Ranch and Superstition Hills events (17), but few aftershocks are seen (18).

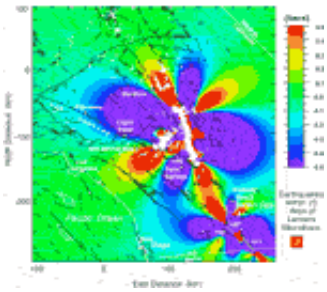

Fig. 3. *Coulomb failure stress changes (μ =0.4) caused by M?6 earthquakes in southeastern California during 1979-1992. Quaternary faults are black; the coastline is white. ML?1 earthquakes within 25 days of the Landers shock are from the Caltech-U.S. Geological Survey RTP network (rms?0.4 s, ?7 arrivals). Most Landers aftershocks*

San Andreas segment boundaries inferred by (19) accord roughly to sign changes in the failure stress change imposed by the Landers event. In Fig. 4A the failure stress change is resolved on the San Andreas fault, rather than on the azimuth of maximum stress change as shown in Figs. 1-3. The calculation for Fig. 4 is independent of the magnitude, uniformity, and orientation of the regional stress, and depends only on fault geometry. The failure stress change is positive in the central Coachella Valley segment,

negative at the segment boundary north of Palm Springs, and is greatest in the San Bernardino Mountain segment (site of a M_L =4.4 aftershock 37 min before the Big Bear shock). All of the Mojave segment is negative (Fig. 4A). The stress change on the northern San Jacinto fault SE of San Bernardino, which is more favorably oriented than the San Andreas, is 1 bar. The predicted stress change resolved on the San Andreas fault increases with μ, since tension normal to the fault is enhanced.

The correspondence between seismicity and the Coulomb failure stress changes produced by the Landers and earlier events suggests that regions of predicted increase are candidates for future major events. To predict how the Landers earthquakes have advanced or delayed the next great southern San Andreas earthquake, we let a frictionless San Andreas slip freely to relieve the stress imposed by the Landers and surrounding earthquakes (Fig. 4B). The immediate response is slip of 20 cm over 30 km of the central San Bernardino segment (equivalent to a M=6.2 event if it occurred seismically), and 7 cm in the northern Coachella Valley segment (equivalent to M=5.7). Thus San Andreas fault slip with a moment equivalent to two moderate events are needed simply to relieve the stresses added by the recent earthquakes. In contrast, a load comparable to a M=6.2 event is removed from the Mojave segment, and a M=6.0 load is removed north of Palm Springs (20), taking these portions of the fault farther from failure. After relaxation of the viscous substrate in our idealized plate model, the stress change on the San Andreas and surrounding faults roughly doubles (Fig. 4A, orange curve), as stress is transferred from the base of the fault back to the upper crust. Similarly, the slip required to relieve the stresses also rises (Fig. 4B, orange fields). The calculated slip does not depend on the number of segments allowed to slip at once. So far no creep has been measured (21) and no moderate earthquakes have occurred on these faults since the Landers event. If these events do not take place, the likelihood of great earthquakes on the San Andreas must rise as well.

are found where the predicted failure stress change is positive. Stress changes caused by the 1979 Imperial Valley (IV), 1987 Elmore Ranch (ER) and Superstition Hills (SH) earthquakes are included, but their aftershocks are not shown. Predicted stress has risen along the Coachella Valley segment (Bombay Beach to north of Indio) and the San Bernardino Mountain segment (North of Palm Springs to Cajon Pass). The Mojave segment (Cajon Pass to west edge of map) has been unloaded. Y=Yucaipa. Other faults shown are Elsinore (EF), San Jacinto (SJF), Garlock (GF), Camp Rock (CRF), Pisgah (PF), Lenwood (LF), and Blackwater (BF). Upper left corner is 36.00°N/119.00°W; lower left corner is 32.50°/115.00°W.

(Click on the diagram to display a large image - 49kb)

Because the southern San Andreas fault is likely late in the earthquake cycle, the long-term probability of a great earthquake on any of its three southern segments was high before the Landers earthquake took place (19). The San Bernardino Mountain segment last ruptured in 1812 (22); given its 24 ± 3 mm/yr slip rate (23), a $\geq$ 4.3-m slip deficit has since accumulated, which could yield a M $\geq$ 7.5 event. The Coachella Valley segment last ruptured in 1680, has a slip rate of 25-30 mm/yr, and thus has accumulated a $\geq$ 6 m deficit (M $\geq$ 7.5). Its prehistoric repeat time is $\geq$ 235 yrs (24). The Mojave segment last ruptured in 1857, has a slip rate of ~35 mm/yr (23), and thus has accumulated a 4.7 m deficit (M $\geq$ 7.7); its repeat time is ~130 years (22). The San Bernardino Valley segment of the San Jacinto fault may have last ruptured in 1890; it has a slip rate of 8±3 mm/yr (19), and thus has a slip deficit of $\geq$ 0.8 m (M $\geq$ 6.8).

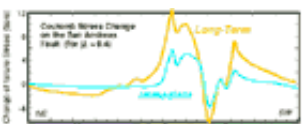

Fig. 4. *(A) Change in the Coulomb failure stress resolved on the San Andreas fault caused by M?6 earthquakes in southeastern California since 1979. Model fault is vertical and passes between the two San*

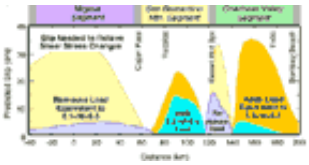

Andreas branches east of Yucaipa. (B) Corresponding slip distribution along the San Andreas fault needed to relieve shear stress imposed by M?6 earthquakes since 1979. Immediate changes are calculated in an elastic halfspace, and so the base of the fault restrains displacement. Long-term changes are calculated in an elastic plate, with upper and lower surfaces stress-free. Induced right-lateral slip (added loads) are solid fields; left-lateral slip (remvoed loads) are stipled.

(Click on the diagram to display a large image - 18kb)

We estimate the advance and delay times of great earthquakes on the San Andreas by dividing the slip required to relieve the applied stress (Fig. 4B) by the local San Andreas or San Jacinto slip rates. The calculation is independent of the great earthquake repeat times or stress drops, for which there is considerable uncertainty. Our estimate is bounded by the difference between the slip predicted for immediate and long-term periods. We find that the next great San Andreas earthquake along the San Bernardino Mountain segment will strike 8-22 years sooner than it would have in the absence of the Landers shock. Similarly, the next great San Andreas earthquake along the Coachella Valley segment is advanced by 2-14 years, and the next large earthquake on the San Bernardino Valley segment of the San Jacinto fault is advanced 8-56 years. In contrast, we estimate a delay in the next great Mojave shock by 2-10 years. An earthquake of $M \geq 6$ on the Mojave segment during the next 2 years would thus falsify our hypothesis.

REFERENCES AND NOTES

1. R. K. Dokka and C. J. Travis, Geophys. Res. Lett. 17, 1323 (1990).
2. J. C. Savage, M. Lisowski, W. H. Prescott, ibid., p. 2113 (1990).
3. A. Nur, H. Ron, O. Scotti, in Slow Deformation and Transmission of Stress in the Earth, S. C. Cohen and P. Vaníc? ek, Eds. (American Geophysical Union, Washington, D.C., 1989), Geophys. Monogr. 49, IUGG Vol. 4, pp. 31.
4. The halfspace program incorporates the elastic dislocation code of Y. Okada (Bull. Seismol. Soc. Amer. 82, 1018, 1992) into the framework of S. L. Crouch and A. M. Starfield, Boundary Elements in Solid Mechanics (Allen Unwin, London, 1983). The plane stress boundary element program [see R. G. Bilham and G. C. P. King, J. Geophys. Res. 94, 204 (1989), and G.C.P. King and M. Ellis, Nature 348, 20 (1990)] runs on Macintosh computers, and is available from King. Poisson's ratio, n, is 0.25 and Young's modulus, E, is 8.8 x 1011 dyne-cm-2.
5. P. A. Reasenberg and R. W. Simpson, Science 255, 1687 (1992).
6. J. R. Rice, in Fault Mechanics and Transport Properties of Rock, B. Evans and T.–F. Wong, Eds. (Academic Press, London, 1992), pp. 475.
7. R. S. Stein and M. Lisowski, J. Geophys. Res. 88, 6477 (1983). The moment used for the Homestead Valley earthquake includes postseismic slip extending through the plate, consistent with measured 1979-81 deformation.
8. D. H. Oppenheimer, P. A. Reasenberg, R. W. Simpson, J. Geophys. Res. 93, 9007 (1988).
9. K. W. Hudnut, L. Seeber, J. Pacheco, Geophys. Res. Lett. 16, 199 (1989); S. Larsen. R. Reilinger, H. Neugebauer, W. Strange, J. Geophys. Res. 97, 4885 (1992).
10. R. W. Simpson and P. A. Reasenberg, U.S. Geol. Surv. Prof. Pap. on the Loma Prieta

Earthquake (in press).
11. M. Lisowski, J. C. Savage, W. H. Prescott, J. Geophys. Res. 96, 8369 (1991) found a principal contractive strain rate of N7±1°E from trilateration surveys conducted since 1979 in the Joshua geodetic network, which includes most of the Landers rupture. J. Sauber, W. Thatcher, S. C. Solomon, J. Geophys. Res. 91, 12683 (1986) found the most compressive principal strain direction measured during 1934-1982 across the north half of the Landers rupture to be N4±5°E from triangulation surveys.
12. L. M. Jones, J. Geophys. Res. 93, 8869 (1988). The mean of the principal stress directions for the two segments that abut the Landers site, Banning and Indio, is N6±2°E. P. L. Williams, L. R. Sykes, C. Nicholson, L. Seeber, Tectonics 9, 185 (1990), found an average principal stress direction for the adjacent 50 km stretch of the San Andreas fault (San Gregorio Pass and Eastern Transverse Range-I regions) is N8±5°E.
13. C. DeMets, R. G. Gordon, D. F. Argus, S. Stein, Geophys. J. Int. 101, 425 (1990). The Pacific-North American plate motion vector for central California is N36±2°W, which yields a principal compression oriented N9±2°W.
14. M. D. Zoback and J. H. Healy, J. Geophys. Res. 97, 5039 (1992). The Cajon Pass well yields a N57±19°E principal stress direction. If permanent, this stress could not drive local right-lateral slip on the San Andreas fault, and has been interpreted to suggest that the San Andreas is a weak (low-m) fault embedded in a strong (high-m) crust (see M. D. Zoback and A. H. Lachenbruch, ibid, p. 4991, 1992). The stress measured in the well may be influenced by local faults (G. Shamir and M. D. Zoback, ibid, p. 5059, 1992) and thus not represent a regional value.
15. All earthquakes in this study except North Palm Springs occurred on near-vertical faults with dominant strike slip. We simulate the 30% dip-slip component and 59° dip of the North Palm Springs rupture by including a fault-closing (eg., dike deflation) displacement equal to cos(rake) x cos(dip). This approximation gives accurate stresses at distances greater than one fault length from the source.
16. The mean static shear stress drop calculated from the parameters in Table 1 following H. Kanamori and D. L. Anderson, Bull. Seismol. Soc. Amer. 65, 1073 (1975).
17. C. E. Johnson and D. P. Hill, in The Imperial Valley, California, Earthquake of October 15, 1979(U.S. Geol. Surv. Prof. Pap. 1254, 1982) p. 15; S. H. Hartzell and T. H. Heaton, Bull. Seismol. Soc. Amer. 73, 1553 (1983); T.C. Hanks and C.R. Allen, Bull. Seismol. Soc. Amer. 79, 231 (1989). K. Hudnut et al., ibid., p. 282 (1989).
18. Landers aftershocks could be absent in the Coachella Valley because the total stress there is lower or because the strength is higher. We examined the effect of a low-modulus Mojave tectonic block embedded in a stiffer crust, consistent with the Pg velocity contours of T. M. Hearn and R. W. Clayton, Bull. Seismol. Soc. Amer. 76, 495 (1986). The average velocity contrast between the 100 x 300 km Mojave region with Pg velocity <6.2 km/s and the surrounding medium is 0.45 km/sec. We gave the Mojave block a Young's modulus, E, of 6.2 x 1011 dyne-cm-2 bars. In this plane stress calculation, the Coulomb failure stress increase is halved in the Coachella Valley, but is nearly unchanged elsewhere. Thus it is possible that we overestimate the stress change for the Coachella valley in Figs. 3 and 4.
19. Working Group on California Earthquake Probabilities, U.S. Geol. Surv. Open-File Rep. 88-398 (1988).
20. Site of the 1948 M=6.0 Desert Hot Spring earthquake; see L. R. Sykes and L. Seeber, Geology 13, 835 (1985).
21. Global Positioning System monitor networks have not detected postseismic slip greater than

several centimeters across the San Andreas fault at Cajon Pass and in the Coachella Valley (M. Lisowski, pers. comm.).
22. G. C. Jacoby, K. E. Sieh, P. R. Shepard, Science 241, 196 (1988); K. Sieh, M. Stuiver, D. Brillinger, J. Geophys. Res. 94, 603 (1989).
23. R. J. Weldon II and K. E. Sieh, Geol. Soc. Amer. Bull. 96, 793 (1985); R. J. Weldon II, Ph.D. thesis, California Institute of Technology (1986).
24. A. G. Lindh, in Earthquake Prediction: Present Status, S. K. Guha, A. M. Patwardhan, Eds. (University of Poona, Pune, India, 1988) pp. 189. Coachella Valley segment repeat times are based on K. E. Sieh (abstract), EOS 67, 1200 (1986).
25. R. L. Hill and D. J. Beeby, Geol. Soc. Amer. Bull. 88, 1378 (1977); A. Lindh, G. Fuis, C. Mantis, Science 201, 56 (1978).
26. N. E. King, D. C. Agnew, F. Wyatt, Bull. Seismol. Soc. Amer. 78, 1693 (1988).
27. J. C. Savage, M. Lisowski, W. H. Prescott, EOS 73, in press (1992).
28. L. M. Jones, K. Hutton, D. A. Given, C. R. Allen, Bull. Seismol. Soc. Amer. 76, 1830 (1986).
29. J. Pacheco and J. Nábelek, Bull. Seismol. Soc. Amer. 78, 1907 (1988); S. Hartzell, J. Geophys. Res. 94, 7515 (1989).
30. C. J. Ammon, A. A. Velasco, T. Lay, Geophys. Res. Lett., submitted (1992).
31. Preliminary broad band measurements of the Landers and Big Bear seismic moments are from H. K. Thio and H. Kanamori, and from G. Ekström (pers. comm.).
32. Fault slip function from preliminary fault mapping by D. Ponti, M. Rymer, K. Lajoie, and from K. Sieh, K. Hudnut, C. Rubin and T. Rockwell (pers. comm.).
33. We thank Amos Nur, Raymond Weldon II, Wayne Thatcher, Lucile Jones, and James Savage for thoughtful reviews, and Robert Simpson and Ruth Harris for stimulating discussion. We are grateful for financial support from the Southern California Earthquake Center.